Multidisciplinary Optimization of an Electric Quadrotor Urban Air Mobility Aircraft

Eric S. Hendricks*, Eliot D. Aretskin-Hariton†, Daniel J. Ingraham‡,
Justin S. Gray§, Sydney L. Schnulo¶, Jeffrey C. Chin‖,
Robert D. Falck**, and Dustin L. Hall††
NASA Glenn Research Center, Cleveland, OH, USA

Urban Air Mobility (UAM) vehicles have the potential to augment urban transportation systems, allowing passengers to skip the congested ground traffic. This emerging market is opening up the design space for a new class of UAM vehicles which could be powered by electric propulsion systems to be economical and environmentally friendly. However, development of these UAM concepts presents several additional challenges in the design process. First, these concept designs require including new disciplinary models for subsystems such as electric motors, cables, batteries and thermal management systems. Second, correctly designing and evaluating these various subsystems requires tight coupling between the discipline models to capture interactions. This paper presents the continued development of a multidisciplinary design optimization environment to aid in the development of these vehicle concepts. The multidisciplinary environment fully couples the various subsystem models allowing for the full vehicle to be designed and optimized simultaneously. In this research, the developed modeling approach is demonstrated in the analysis of a small, all-electric quadrotor UAM concept. Results from these studies show that numerous disciplines can be tightly coupled and producing improved overall vehicle designs.

Nomenclature

$\bar{X}$	design variable vector
$\bar{Y}$	design output vector
BEMT	blade element momentum theory
HX	heat exchanger
ISA	Intenational Standard Atmosphere
NDARC	NASA Design and Analysis of Rotorcraft
RVLT	Revolutionary Vertical Lift Technology Project
SOC	state of charge
TMS	thermal management system
TTT	Transformative Tools and Technologies Project
UAM	Urban Air Mobility
VTOL	vertical takeoff and landing
XDSM	eXtended Design Structure Matrix

*Aerospace Engineer, Propulsion Systems Analysis Branch, 21000 Brookpark Rd MS 5-11.
†Aerospace Engineer, Intelligent Control and Autonomy Branch, 21000 Brookpark Rd MS 77-1.
‡Aerospace Engineer, Acoustics Branch, 21000 Brookpark Rd MS 54-3.
§Aerospace Engineer, Propulsion Systems Analysis Branch, 21000 Brookpark Rd MS 5-11, AIAA Member
¶Aerospace Engineer, Propulsion Systems Analysis Branch, 21000 Brookpark Rd MS 5-11.
‖Aerospace Engineer, Propulsion Systems Analysis Branch, 21000 Brookpark Rd MS 5-11.
**Aerospace Engineer, Mission Analysis and Architecture Branch, 21000 Brookpark Rd MS 162-2, AIAA Member.
††Aerospace Engineer, Propulsion Systems Analysis Branch, 21000 Brookpark Rd MS 5-11.

I. Introduction

A new class of aircraft concepts with a combination of vertical takeoff and landing (VTOL) and electrified propulsion systems are being proposed to fulfill an emerging market for Urban Air Mobility (UAM). This market, centered in densely populated urban areas, would provide air taxi services over short distances (less than 100 km) such that passengers could avoid congested surface streets below. In the near term, the concept of operations would likely see these aircraft operate out of vertiports on scheduled routes with longer term market growth into flexible point-to-point flights.[1] While a widespread market for these flights does not currently exist, it is projected that there could demand for 55,000 daily flights carrying 82,000 passengers in the near term.[2] Such a demand would create a market value of approximately $2.5 billion and require upwards of 4000 air taxi vehicles.[2]

This potential market has generated significant interest among a variety of traditional and start-up aircraft manufacturers and operators. While existing helicopters could fill this market, advancements in technology coupled with shorter intra-urban missions have opened the design space for unconventional VTOL designs. Furthermore, it is hoped that these unconventional systems will enable a safe mode of transportation as well as have better operating costs and reduced environmental impact (in terms of both emissions and noise) compared to conventional helicopters. With these design objectives and a large potential market, a number of potential UAM vehicle concepts have been proposed by industry as well as by NASA's Revolutionary Vertical Lift Technology Project (RVLT).[3,4] The vehicles proposed by NASA, shown in Fig. 1, have been put forward as a means to identify design and technology challenges which will focus ongoing research to enable development of viable UAM commercial vehicles.[3]

Figure 1: NASA UAM Concept Vehicles.

Given these goals, NASA's RVLT project developed their UAM concept vehicles using existing rotorcraft design and analysis tools. These codes modeled the major systems needed for all VTOL aircraft and used simple assumptions for many of the unconventional subsystems such as electrical components and thermal management system (TMS). The codes and assumptions were then implemented as part of a traditional design process where limited coupling was considered between the subsystem designs. This process worked well for the main objective of refining the designs to the point that they could be used in identifying design needs and guiding the technology research. However, as part of this study it was identified that the traditional design process needed to be modified to perform an integrated multidisciplinary environment to optimize these concepts to further improve the overall design.[3]

To address this need, a research effort was started under NASA's Transformative Tools and Technologies Project (TTT) to explore the development of an improved multidisciplinary design capability. This capability aimed to include more detailed models for many of the unconventional subsystems and tightly couple these disciplinary models together to capture interactions between subsystems as part of the conceptual design process. In particular, the research sought to apply gradient-based optimization algorithms to efficiently explore the complex design space for these new UAM vehicles. The development of the multidisciplinary design environment therefore focused on applying tools which could provide fast and accurate analytic derivatives to the optimization algorithms. The newly developed multidisciplinary design capability and supporting subsystem analysis tools were presented by Hendricks et al.[5] with the environment demonstrated in the study of the tiltwing concept shown in Fig. 1. The work was later expanded to more thoroughly model

the turboelectric propulsion and thermal management systems of the vehicle.[6] The results presented in both of these studies showed the value of tightly coupling the subsystem analyses as part of a multidisciplinary design process and revealed interesting trade-offs between the subsystem designs.

The research work presented in this paper continues to refine this multidisciplinary design capability for UAM concept vehicles and applies it to a different vehicle concept. In the present study, the smallest of the NASA concept vehicles shown in Fig. 1 was selected. This vehicle is a quadrotor concept (shown in more detail in Fig. 2) designed to carry a single passenger up to 92km (50nm). Given this short range and relatively small payload, the initial conceptual design proposed an all-electric, battery powered vehicle. For this concept, the battery and thermal management systems present a challenging design problem as they require coupling with the rest of the vehicle subsystems to ensure valid designs are generated. In addition, the dynamic behavior of these systems is of primary importance necessitating that the entire mission analysis be included as apart of multidisciplinary assessment. The research presented in this paper therefore focuses heavily on the designs for these systems as well as the overall dynamic operation of the vehicle.

Figure 2: NASA UAM Quadcopter Concept Vehicle.

This paper is organized as follows: Section II will review the multidisciplinary optimization approach previously presented by Hendricks et al.[5] and applied to the tiltwing UAM concept vehicle. The section will also present the revised multidisciplinary environment created specifically for assessing the quadrotor concept including descriptions of all the subsystem models which are part of the analysis. Following this overview of the modeling environment, Section III presents the application of the developed capability to the quadrotor vehicle. Several different optimization studies were conducted and the results are used to evaluate the design trade space for this concept. Lastly, conclusions and future research directions are discussed in Section IV.

II. Multidisciplinary Analysis Environment

As described in the Introduction, many of the UAM concepts being proposed use new technologies such as electrified propulsion systems to address operational cost and environmental impact goals for these vehicles. Development of these conceptual designs, however, has often relied on the use of a traditional design process centered around the use of a suite of well established modeling tools. While these tools have been used extensively for traditional rotorcraft, they lack some of the disciplinary models necessary for these unconventional UAM configurations and propulsion systems. Furthermore, the typical design process can be described as an iterative sequential design optimization approach. In this type of approach, each of the disciplinary models are designed and analyzed independently with limited sharing of design information between the disciplinary engineers or their models. Instead, each of the subsystem models (such as the engine or rotor) typically produces performance tables for a specific design. This tabulated data is then used to evaluate the overall performance of the vehicle and determine if the design closes to a converged state. This process can require a number of manual iterations through each of the subsystem designs when the design fails to close or if better vehicle level performance is desired.

Given these limitations, the previous research of the authors developed a revised conceptual design ap-

proach.[5] This approach focused on providing tight coupling between the various subsystem models enabling interactions between the subsystems to be captured in the vehicle design. The tightly coupled approach, where all required information is automatically passed between disciplinary models, also allows for the optimization of the overall vehicle to be completed with limited manual interaction.

A high-level view of this revised design methodology is shown in the eXtended Design Structure Matrix (XDSM)[7] shown in Fig. 3. This diagram depicts the high-level model components, execution sequence, and more importantly the data which couples the various components to form a tightly integrated analysis process. In this figure, the main analysis is broken up into three primary elements shown along the diagonal. The first element is a gradient based optimizer which drives the execution of the various models by altering design and control variables to achieve a target design objective subject to a set of constraints. The second element comprises the design calculations for all disciplinary models included in the analysis. The models in this part of the design process size each of the vehicle subsystems based on the most demanding flight condition and thereby determine the overall size and mass of the vehicle. The disciplinary design characteristics determined in this part of the methodology are then passed to the mission performance analysis element. This part of the analysis evaluates the performance of the overall vehicle design developed in the first phase throughout an entire flight profile to determine if mission performance requirements are satisfied. The analysis results from both the disciplinary design and mission performance elements are then fed back to the optimization algorithm until a final solution is identified. The following paragraphs will describe the details of the disciplinary design and mission performance elements which were specifically implemented for the electric quadrotor vehicle being studied in the paper. Details of the individual disciplinary models developed for this vehicle are also presented later in this section.

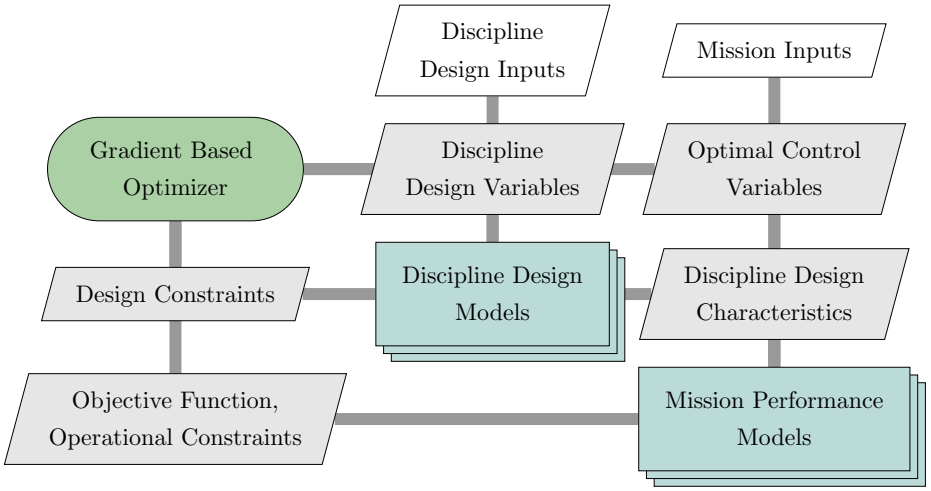

Figure 3: Multidisciplinary Design and Analysis Environment.

The disciplinary design environment, shown in Fig. 4, develops the design for each of the major aircraft subsystems based on the performance requirements at the most demanding flight condition. The design environment starts by determining important flight condition parameters such as thrust requirements and atmospheric properties. Following these steps, the main portion of the disciplinary design phase works through the entire propulsion system starting at the rotors then moving to the electric motors, cables, and batteries. For each component in the propulsion system, the models are coupled by passing the power required from the upstream component in the power train. These models also take in design inputs that are either set as constants by the user or allowed to vary as part of the optimization process as shown by the white and gray parallelograms in the top two rows of the figure. Following the main power train elements, the thermal management system is sized in the design process to determine its mass. Finally, the entire aircraft mass is computed based on the outputs from the various subsystems as well as empirical models for other elements of the vehicle (such as the fuselage, landing gear, etc.) which were not explicitly modeled. The results of this entire disciplinary design portion of the environment are the design characteristics of each of the subsystems as well as the overall vehicle size. These design outputs, shown in the white parallelograms on the right, are then passed on to the mission performance analysis element of the design process.

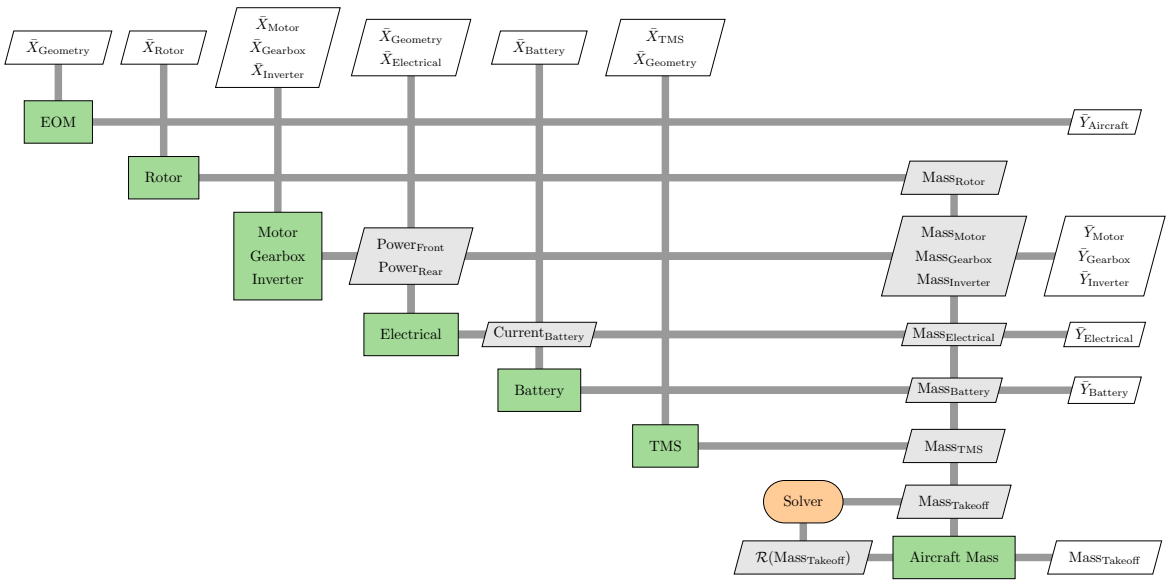

Figure 4: Discipline Design Integrated Model.

The second portion of the model takes the vehicle design and evaluates its performance throughout an entire mission. This part of the analysis includes many of the same disciplines as the design portion, but executes them dynamically throughout the entire flight to determine their performance characteristics at all time steps. The mission analysis portion of the MDAO environment is actually split into two separate coupled phases which are executed in tandem. The main phase captures the performance characteristics of the propulsion systems as well as the overall vehicle trajectory. As shown in Fig. 5, the analysis includes the same subsystem models for the propulsion system components. This section does include an additional solver to converge the voltage between the battery and the rest of electrical system as the voltage of the battery changes with state of charge (SOC) and therefore impacts the electrical transmission properties. In addition, the main phase includes models for the body forces on the vehicle and the equations of motion which are needed to determine the performance characteristics of the quadrotor in flight. Within the main phase, the discretization with time is relatively coarse to enable rapid model execution while still providing accurate results.

While the main phase of the mission performance modeling element models the propulsion system and vehicle performance, a separate phase was created specifically for the TMS as shown in Fig. 6. This model is separated from the rest of the mission analysis as it allows for a finer time discretization to capture the transient temperature changes occurring in the TMS components. While they are modeled in separate phases, the main phase and TMS phase are tightly coupled with the component temperatures and power required to run the TMS system connected between the phases. In combination, these two separate phases allow for the entire mission performance of the vehicle to be determined at appropriate time discretizations for each subsystem.

The paragraphs above broadly describe the various elements of the overall MDAO design environment constructed to model the all-electric quadrotor UAM vehicle. Implementation of this approach however requires models for each of the disciplines as well as a means to couple them together, evaluate them dynamically as part of a mission analysis, and run an optimization to explore the design space. For this research, the entire multidisciplinary design environment was constructed using OpenMDAO.[8] OpenMDAO is a multidisciplinary optimization framework that provides several valuable features. First, it can combine multiple disciplinary analysis codes into a single coupled model and manages the data connections and execution of each code. It also contains a suite of numerical solvers and optimizers which can easily be implemented on a variety of problems and models. Lastly, for gradient-based optimization methods, it provided a means for combining individual disciplinary derivatives into the coupled derivatives needed for gradient based optimization.[8] In addition to OpenMDAO, the time dependent modeling in the mission performance portion of the environment was enabled by use of the Dymos library.[9] Dymos, which is built on top of OpenMDAO, is a flexible framework for simulation and optimization of dynamical systems that

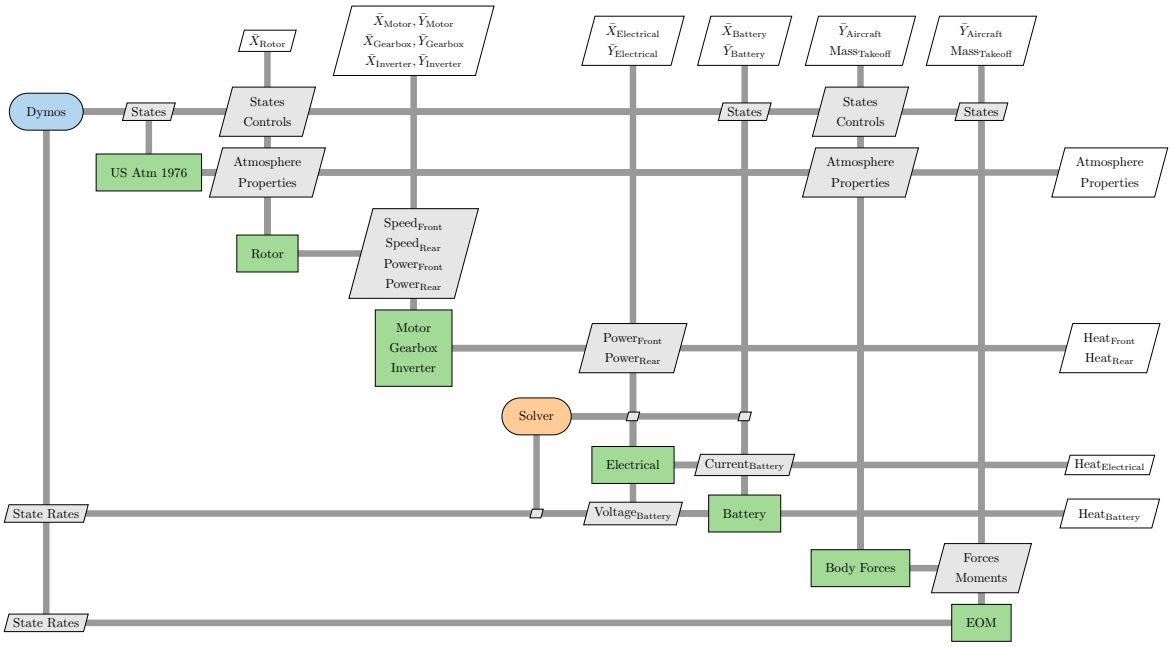

Figure 5: Mission Performance Modeling Phase.

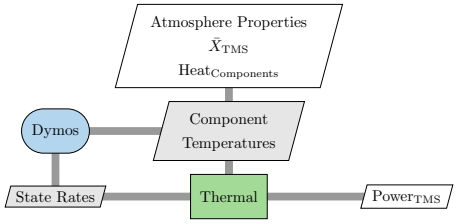

Figure 6: Thermal Management Modeling Phase.

provides a generic ordinary differential equation integration capability and enables solving optimal control problems. Overall, both of these tools provide key foundational capabilities for developing the overall tightly coupled UAM MDAO capability. The various disciplinary analysis tools used to model the vehicles therefore were developed to work with these frameworks (and in many cases were built on top of OpenMDAO). Details of the disciplinary analysis tools used in this study are provided in the following subsections.

A. Rotor

The purpose of the rotor model is to map the rotor blade properties, the vehicle's state, and a target thrust to a rotor rotation rate and shaft power for each point in the trajectory. For the analysis of the quadrotor in this study, the modeling approach used a version of blade element momentum theory (BEMT). Please see references[10–13] for more details on BEMT theory, and especially Ning[14] for the specifics of the BEMT calculations used here.

The BEMT implementation used in this research is `CCBlade.jl`,[15] a new version of the National Renewable Energy Laboratory's CCBlade[16] code written in the Julia programming language.[17] `CCBlade.jl` has been carefully designed to be both **C**ontinuous and **C**onvergent, which makes it especially amenable to large-scale gradient-based optimizations. The BEMT equations are solved using the Brent solver from `FLOWMath.jl`,[18] and the derivatives are computed analytically using the automatic differentiation library `ForwardDiff.jl`.[19]

`CCBlade.jl` is shown in the context of the complete quadrotor rotor model in Figure 7. The inputs to the rotor model are shown in the white parallelograms at the top of the figure. These include chord and twist variables which serve as control points for defining the chord and twist distributions along the blade. It

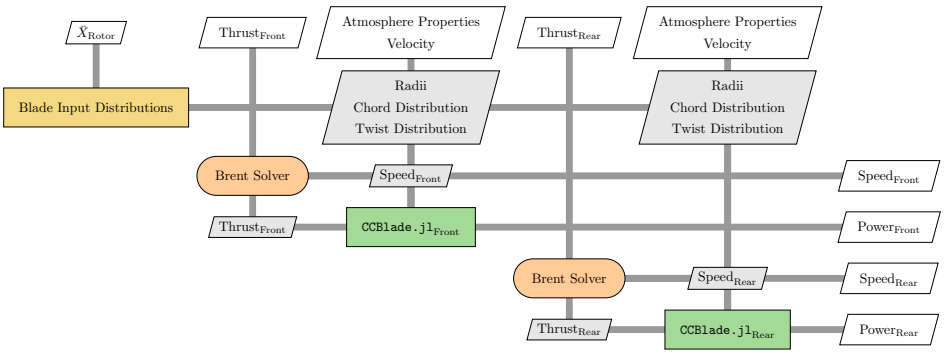

Figure 7: XDSM for the Rotor Model.

should also be noted that the velocity input for the rotor analysis is the component of the vehicle's velocity normal to the rotor rotation.

The first step in the rotor modeling process is the "Blade Input Distributions" object which is a preprocessing step completing several tasks. First, it creates an evenly spaced grid of radial locations that serve as the positions of the BEMT blade elements (the radii variable in Figure 7). Second, the object assigns a value for the chord and twist at each of the blade elements by interpolating the chord and twist control points onto the Radii grid (Chord Distribution and Twist Distribution).

The radii, chord, and twist variables are then passed to the two `CCBlade.jl` components, along with the atmosphere properties and velocity, as well as shaft speed estimates for the rotors' rotation rate from a Brent solver. (The Brent solvers in Figure 7 are separate from those internal to the `CCBlade.jl` components, which are not shown.) `CCBlade.jl` then calculates the rotor thrust from those inputs, which is fed back into the Brent solver. The Brent solver updates the shaft speed, and this process continues iteratively until the thrust calculated by `CCBlade.jl` matches the input target value. Finally, shaft speeds and power values are sent downstream to the motor model.

In addition to these performance calculations, the rotor model estimates the mass of the subsystem in the disciplinary design environment. The rotor mass calculations follow the empirical AFDD82 model used by NASA Design and Analysis of Rotorcraft (NDARC)[20] and includes blade, hub, spinner, and fold weight.

B. Motor

The motor block shown in Figures 4 and 5 models the electric motors required to drive each of the rotors as well as two associated components: the gearbox and electrical inverter. These systems were combined together in this grouping given their coupled design requirements and operational behavior.

For the electrical motor, the model in the present study captures changes in motor performance based on a relatively simple efficiency map. This map computes the efficiency as a function of shaft speed with the maximum efficiency of 97.4% occurring at 2000 rpm. The efficiency decrease at higher or lower speeds followed a parabolic curve, with the efficiency values reaching 74.3% at both 1000 and 3000 rpm. In the disciplinary design portion of the environment, the motor weight was also calculated based on a linear regression of existing aviation specific inrunner motors. This approach is similar to the previous analysis of the tiltwing UAM concept.[5]

In addition to the motor, a simple gearbox was modeled as a means to enable the rotor and motor to operate at their most efficient speeds. As mentioned above, the motor peak efficiency occurred at 2000 rpm. For the rotor, the speed was a design variable controlled by the solver resulting in the gear ratio being calculated in the disciplinary design portion of the analysis. This gear ratio was then held fixed throughout the mission performance assessment along with a constant gearbox power transmission efficiency of 99%. Lastly, the weight of the gearbox was determined based on a linear regression model using a state-of-the-art technology level.[21]

Finally, the motor group also includes the power inverter required to convert DC power coming from the transmission lines to the AC power required by the motor. Again, a relatively simple inverter model was used in this study with a constant 98% power conversion efficiency assumed.

As noted for each of the components in this model, power losses were captured using relatively simple efficiency metrics. This information not only ensured increased power would be needed from the battery,

but also provided a simple model for the waste heat that would be produced by these components. In this analysis, the waste heat generated from these three closely coupled components was passed as a single value to the TMS system and all three components were assumed to be at the same temperature.

C. Electrical Cables

The electrical cables required to transmit power from the battery to the motors, thermal management system and auxiliary loads were modeled using Zappy.[22] Zappy is an object-oriented load (power) flow analysis library developed on top of OpenMDAO for use within aircraft optimization studies. It provides the ability to examine both AC and DC systems with only the DC analysis being used in this analysis.

To model the electrical cables for the quadrotor concept vehicle, a representative electrical system diagram was developed as shown in Fig. 8. The system includes four loads to represent each of the motor subsystems which are attached to the main battery bus through a set of transmission lines (represented in the figure as a single line diagram). In addition to these motors, loads were also included for powering the thermal management system as well as auxiliary systems such as avionics. For the motors and TMS, the load requirements were determined directly from those subsystem models throughout the flight profile to ensure a complete capturing of power loads needed for the battery. For the auxiliary load, this was assumed to be constant throughout the entire flight at 2kW. Finally, the battery was modeled as a simple DC generator in the load flow analysis and was coupled to the detailed battery model described in the next section. This coupling ensured that the battery voltage and power demanded by the entire vehicle were being provided by the battery at each point in the flight.

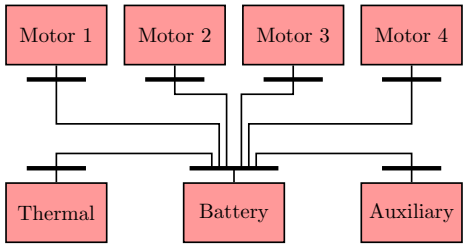

Figure 8: Electrical Power Distribution System.

The electrical system model also included a simple cable sizing methodology to capture effects due to changes in line resistance and mass. To determine these values, the electrical module accepted cable lengths between the various components as inputs. The cable ampacity, weight-per-length and resistance-per-length were also included as inputs such that the model could properly capture changes in the cable design as a function of power and current requirements coming from other subsystems. For this analysis, inputs consistent with standard copper cables were used but these parameters could be used in future studies to examine different cable options if desired. However, different cable materials were studied in a previous paper[23] showing the tradeoffs available from this material selection.

D. Battery

The battery model implemented in this study uses a relatively complex representation of the battery by considering both the cell and pack level design and performance characteristics. The modeling approach is derived from previously conducted research[24] using experimental cell testing performed at NASA Glenn Research Center to accurately capture performance capabilities. While the previous research used 18650-30Q Li-Ion cells, characteristics from Amprius prismatic cells are used in this model. However, in order to match the battery technology factor originally proposed for the reference vehicle[3] the mass of the cells is artificially lowered such that the energy density is 650 Wh/kg at the cell level and 400 Wh/kg installed and usable at the pack level. The 400 Wh/kg metric includes knockdowns for additional pack weight, cell discharge efficiency, and assumes only 80% of the battery energy is usable. To achieve this energy density, the cell mass was reduced from 31.6 to 15.55 grams representing a significant advancement of the current state-of-the-art. More realistic energy density values were also considered in this study, with 350 Wh/kg and 300 Wh/kg energy densities producing cell masses of 17.78 grams and 20.75 grams respectively.

Using these design assumptions, the battery model in the design portion of the environment provides

initial battery sizing calculations. These calculations determine the number of cells in series and parallel based on the design bus voltage, discharge rate, and total energy capacity required. Given that battery efficiency is dependent on the power profile, a conservative efficiency is initially used and then adjusted as needed. To determine the number of cells in parallel, several battery design metrics and constraints are considered. The first examines a power limited condition in which the individual cell discharge reaches it's allowable limit. Meanwhile, the second scenario examines an energy limited state where the total energy capacity of the battery is the limiting factor. Since the limiting constraint is not known a-priori to sizing, both energy and power calculations are used to compute two different parallel battery string sizes. An equality constraint with a solver is then used to ensure both of these calculations match, by varying the allowable discharge rate between lower and upper bounds established by the cell manufacturer. In the energy constrained scenario, the allowable discharge rate will decrease until the problem effectively becomes equally power constrained. In the power constrained scenario, the allowable discharge rate increases until it hits the maximum allowable discharge and only the power method is needed to size the parallel string.

In the mission performance portion of the environment, the battery analysis employs an equivalent electrical circuit model. By using this approach, the components modeling the battery enable the battery performance to vary with both SOC and cell temperature. This model captures variations in open-circuit voltage as well as polarization resistance to characterize voltage drop across any SOC and current draw. To get the cell level performance, the model converts the pack level current draw down to the cell level, then computes performance at the cell level assuming consistent performance across every cell. From the cell level information, the analysis can then calculate the total pack voltage and pack efficiency. Finally, the pack voltage is converged with the assumed value in the upstream cable model to ensure all upstream components match the same voltage as output by the battery model.

E. Thermal Management System

The electric components and batteries described in Sections II.C and II.D, respectively, require a TMS. Each of these components produces waste heat as a result of their inefficiencies and must stay within their temperature limits throughout the flight. The TMS design therefore effects the overall aircraft performance by requiring additional weight and power. In this research, a library developed by Chapman, et. al.[25] was used in order to size the TMS and model the temperatures of the components throughout the trajectory. The architecture of the assumed TMS for the quadrotor vehicle is shown in Fig. 9.

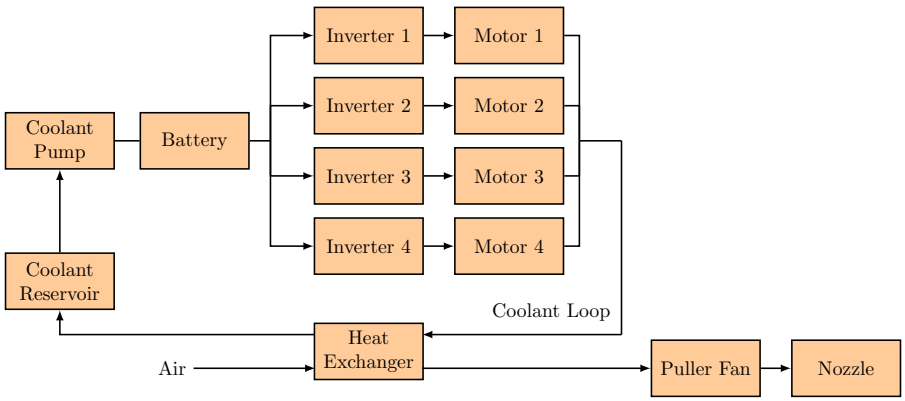

Figure 9: Thermal Management System.

The TMS consists of a liquid loop that is cooled by air via a cross flow heat exchanger. The coolant liquid is assumed to be a propylene glycol water mixture. Each component is transiently modeled as a lumped mass that transfers heat to the coolant through a cold plate with constant effectiveness and pressure drop. The coolant loop first cools the battery pack, as it has the lowest temperature limit, nominally at 50°C. From there, the flow splits into 4 parallel lines, which run through each inverter and its corresponding motor. The motors and inverters are modeled as one lumped mass with a temperature limit of 90°C. Because the flight dynamics are one-dimensional, the power level (and therefore temperature) of the two front motors will be equal, and the same holds true for the rear motors. Consequently, only one front motor and one rear motor are tracked as a temperature state. The coolant flow coming out of all of the motors is combined and goes

through the fluid side of the air-coolant heat exchanger. A puller fan pulls air through the heat exchanger which is exhausted through a nozzle. The effectiveness and pressure loss of the heat exchanger is calculated conventionally assuming a plate-fin architecture. A coolant reservoir is included to account for the thermal mass of the coolant itself, as well as a coolant pump.

The TMS model estimates the mass, power, and drag it incurs on the aircraft. The mass, computed in the disciplinary design portion of environment, includes the air-coolant heat exchanger, coolant lines, coolant, coolant pump, fan, and nozzle. It is assumed that the cold plate interfaces are included in the electric component weights. In the mission performance model, the system calculates the temperature rise in the batteries, motors, cables, and coolant, which is then integrated into a temperature time history. The model also computes power required by the TMS to run the fan and the coolant pump at each time step in the flight trajectory. This power must be provided by the battery, therefore informing the battery power requirements and sizing. The design variables in the TMS are the coolant flow rate, the coolant reservoir mass, the lengths of the coolant and air side of the heat exchanger, the width of the heat exchanger, and the nozzle throat area, which affects the air flow rate. The component temperatures are constrained throughout the mission, which ensures that the size of the TMS is sufficient.

F. Flight Dynamics

To model the flight dynamics of the quadrotor aircraft in the mission performance environment, two components were created which capture the body forces and equations of motion. Together, these components implement a 6-degree of freedom model based on the equations described by Beard.[26] This formulation uses position, velocity, body rotation rates, and body-to-inertial rotation angles as states to describe the system. The forces from thrust, gravity, and drag are combined with the vehicle moment of inertial to create a summation of forces and moments for each axis. These values and small angle approximations allow for the calculation of state rates.

The equations of motion for this quadrotor study were further simplified as the flight profile only considered two dimensions: vertical and horizontal. Combined with the assumed symmetric aerodynamic profile of the vehicle along each axis, this allowed for the removal of two rotational states. Therefore, the model allowed the vehicle to pitch forward and backwards but prevented the vehicle from yawing or rolling. As a result, the number of states for the system after simplification was reduced to four translational states and two rotational states.

With these equations of motion, the trajectory was modeled as a single phase within the Dymos code. This phase was constrained by applying state boundary conditions including zero velocity and zero pitch angle at the end of the mission. At the start of the mission, however, the initial pitch and pitch rate were left unconstrained to decrease numerical oscillations that were observed in the resulting flight profile. Throughout the mission, this pitch angle was limited to 15 degrees and the pitch rate was constrained to 0.1 degree per second to reduce oscillations in the trajectory results. The moment of inertial and drag forces of the vehicle required for these calculations were determined by assuming a spherical fuselage. Furthermore, the descent velocity was limited to 5m/s to ensure that the rotors were always providing thrust and not in an autorotation or windmill state.

G. Aircraft Mass

The last model in the disciplinary design environment computes the total aircraft mass based on the individual masses of each major vehicle subsystem. As described in the previous disciplinary modeling sections, each of the subsystems for the power train and TMS estimated their individual masses based on determined design characteristics. These masses were supplemented with other major vehicle component masses not explicitly modeled, including the fuselage, landing gear, instrumentation, and passenger/payload.

For these subsystems, a set of empirical correlations or fixed mass assumptions were used similar to those applied in the NDARC code.[20] Specifically, the fuselage model follows the AFDD82 helicopter body weight equation which are based on the wetted area of the fuselage and crashworthiness requirements. For the landing gear, four assemblies were assumed with the model predicting the landing gear mass primarily as a function of takeoff mass. The instrumentation model contains numerous systems including the flight controls, instruments, electrical, avionics, furnishing, environmental, and anti-icing. Since none of these systems change in weight over the sizing routine, a static value of 84.55kg (186.4lb) was assumed. Finally, a mass of 113.4 kg (250 lbs) was assumed for the single passenger/payload in this vehicle.

While computing the overall vehicle mass seems like a simple summation of subsystem masses, this calculation is more complex requiring an iterative procedure. This partially results from the fact that the

fuselage and landing gear masses are a function of the takeoff mass. In addition, any increase in the vehicle mass must be accompanied by an increase in motor size and power, ultimately propagating back to a larger energy requirement in the battery. As a result, an iterative solver must be included within the aircraft mass element to capture an inherent growth spiral.

III. Electric Quadrotor Optimization Demonstration Problem

To demonstrate the capabilities of the MDAO environment, the quadrotor vehicle with the aforementioned subsystems was evaluated as part of a number of optimization studies. These studies examined the impact of various design inputs, performance requirements, and operating constraints. While the details of each optimization varied slightly, a nominal set of mission requirements were generally adhered to in each study. For this quadrotor concept, the nominal design mission was to carry a single passenger 92.6 km (50 nm) on a single battery charge, with a minimum battery SOC of 20% at the end of the flight. Over this mission, the optimal trajectory was determined as part of the optimization within a set of constraints. First, the design mission was simulated in a high elevation urban area with takeoff and landing occurring at 1524 m (5000 ft) altitude. The aircraft was required to climb to a minimum cruise altitude of 1700 m (5577 ft) while also staying below a maximum altitude of 3048 m (10,000 ft). For this initial study, no static hover condition was required and battery reserves for diversion to an alternate airport were not included. (Note that these requirements are different than the nominal mission assumed by Johnson et al. and therefore will lead to a different vehicle design.) Second, the mission was simulated on a hot day relative to the Intenational Standard Atmosphere (ISA), with temperatures of ISA+20 °C (ISA+36 °F). With these high ambient temperatures, the aircraft subsystems were assumed to start the flight at 35 °C with the battery being limited to operation below 50 °C and coolant in the system limited to a maximum temperature of 150 °C. These constraining temperatures were tracked throughout the mission and were important for sizing the TMS.

With these major design and operational characteristics, a formal optimization problem statement was developed as shown in Table 1. For the studies completed in this paper, two different objective functions were considered as shown in the top section of the table. The first potential objective aimed to minimize the takeoff mass of the aircraft as this roughly correlated with the acquisition cost of the vehicle. The second option for an objective function aimed to minimize the energy consumed by the vehicle throughout the flight, which correlates with vehicle's operating cost.

The second section of Table 1 lists out the design variables considered across all the optimization studies. These variables include key design characteristics of many of the subsystems as wells as parameters defining their operational behavior. By including both subsystem sizing variables and operational control parameters, the optimization is able to determine the best combination of vehicle design, trajectory, and control schedule to achieve the target mission.

The subsystem design parameters are listed first, with these variables being a single, scalar value as indicated by the size column (for the rotor blade twist, 6 control points were used to vary the twist along the span). In addition, there were several slack variables which were used by the optimizer to satisfy constraints and make coupling the main phase and TMS phase together easier. For the operational control parameters, this problem allowed for independently varying the front and rear rotor thrust levels at 45 points each throughout the trajectory giving a total of 90 control values.

The third section of Table 1 lists the constraints applied as part of the optimization. Many of these constraints were applied throughout the mission performance calculations. The size column in Table 1 indicates the number of points at which these constraints were applied. Most of the constraints at the top of this section are limits on the physical performance of the quadrotor in flight and include limits on the aircraft trajectory/maneuvers, battery performance, and component temperatures. In addition to these physical constraints, the optimization problem was formulated with constraints for the slack variables added to the problem. Two of these constraints ensured the design vehicle mass and battery characteristics matched those in the mission performance analysis. The other two slack constraints were for the TMS power and battery temperature, which were used to ensure consistency between the main phase and TMS phase in the mission performance analysis. Finally, a large number of pseudospectral constraints are applied as part of the Dymos model to ensure valid results are generated. In total, the optimization problems evaluated in this work considered a relatively large, yet constrained, design space with 256 design variables and approximately 3700 constraints.

Table 1: Optimization Problem Statement.

	Variable/Function	**Size**
minimize	Takeoff mass, or	
	Energy consumption	
with respect to	Total battery energy	1
	Discharge rate	1
	Blade twist distribution	6
	Design rotor power	1
	Coolant flow rate	1
	Heat exchanger width	1
	Heat exchanger height (Coolant)	1
	Heat exchanger height (Air)	1
	Heat exchanger throat area	1
	Takeoff mass (slack)	1
	Rotor shaft speed (slack)	1
	Battery temperature (slack)	75
	TMS power (slack)	75
	Rotor thrust (front and aft)	90
subject to	Time duration	4
	Body frame velocity rates	4
	Max. rotor power	75
	Aircraft pitch rates	76
	Trajectory constraints	154
	Max. descent rate constraint	75
	Min. cruise altitude	45
	Min. battery state of charge	77
	Min. battery Thevenin voltage	75
	Max. battery temperature	271
	Max. coolant temperature	271
	Max. motor temperatures	272
	Takeoff mass (slack)	1
	Battery design constraint (slack)	1
	TMS power (slack)	75
	Battery temperature (slack)	75
	Pseudospectral constraints	2148

Using the problem formulation described this section, a number of design studies were completed on the quadrotor vehicle to explore the multidisciplinary design space. Each of these design studies explored changes in a key mission requirement or design assumption including mission range, maximum allowable battery temperature, battery energy density, and rotor diameter. The next two sections will provide details of the mission range and maximum allowable battery temperature studies completed with this optimization problem. Results for the battery energy density and rotor diameter studies were less insightful and are provided in the Appendix.

A. Mission Range Design Study

In the first design optimization study, the two objective functions described in Table 1 were both considered along with the impact of mission range. Specifically, a shorter range mission of 60 km (32.4 nm) and a longer range mission of 120 km (64.8 nm) were evaluated in addition to the nominal 92.6 km (50 nm) mission. A summary of the vehicle design characteristics which resulted from these six optimizations are provided in Table 2 with some of the mass trends shown in Fig. 10. As expected in these results for both objective functions, the overall aircraft mass increases approximately linearly with increases in range. As observed in the second plot in Fig. 10, this is predominantly because the battery mass also increases linearly to carry the required total energy for the mission. However, there are also secondary impacts from range increases on the electric motor and TMS sizing as shown in the bottom two plots. As the aircraft gets heavier with increased range, a larger, more powerful motor is also required to lift the aircraft. Surprisingly, the larger aircraft (bigger battery and motors) generally results in a slight decrease in the TMS mass. This effect results from the larger battery being more efficient and discharging at a lower rate, thereby producing less heat which needs to be dissipated.

These trends are similar for both the minimum energy and minimum mass objective functions as shown by the solid and dashed lines in Fig. 10. Despite this similarity in trends, there are some relevant differences

Table 2: Vehicle Design Characteristics at Different Mission Ranges.

System	Parameter	Min. Energy 60km	Min. Mass 60km	Min. Energy 92.6km	Min. Mass 92.6km	Min. Energy 120km	Min. Mass 120km
Vehicle	Range, km	60.0	60.0	92.6	92.6	120.0	120.0
	Takeoff Mass, kg	416.72	414.08	467.07	465.23	520.50	519.02
Battery	Max Temp, °C	49.85	49.85	49.85	49.85	49.85	49.85
	Total Energy, kWh	31.51	32.08	51.56	52.09	72.68	73.14
	Max Cell Discharge, A	5.83	5.31	4.21	3.95	3.49	3.33
	Energy Density, Wh/kg	400	400	400	400	400	400
	Mass, kg	62.97	64.12	103.04	104.10	145.24	146.17
TMS	Max Power, kW	0.62	0.89	0.57	0.76	0.59	0.75
	HX Width, m	0.259	0.168	0.233	0.167	0.234	0.181
	HX Height (Coolant), m	0.027	0.026	0.027	0.026	0.027	0.026
	HX Height (Air), m	0.500	0.500	0.500	0.500	0.500	0.500
	Mass, kg	8.52	6.97	7.98	6.82	7.94	6.99
Motors	Shaft Power, kW	11.92	10.96	14.21	13.40	16.73	16.01
	Mass, kg	3.72	3.52	4.20	4.03	4.73	4.58
Rotors	Diameter, m	3.66	3.66	3.66	3.66	3.66	3.66

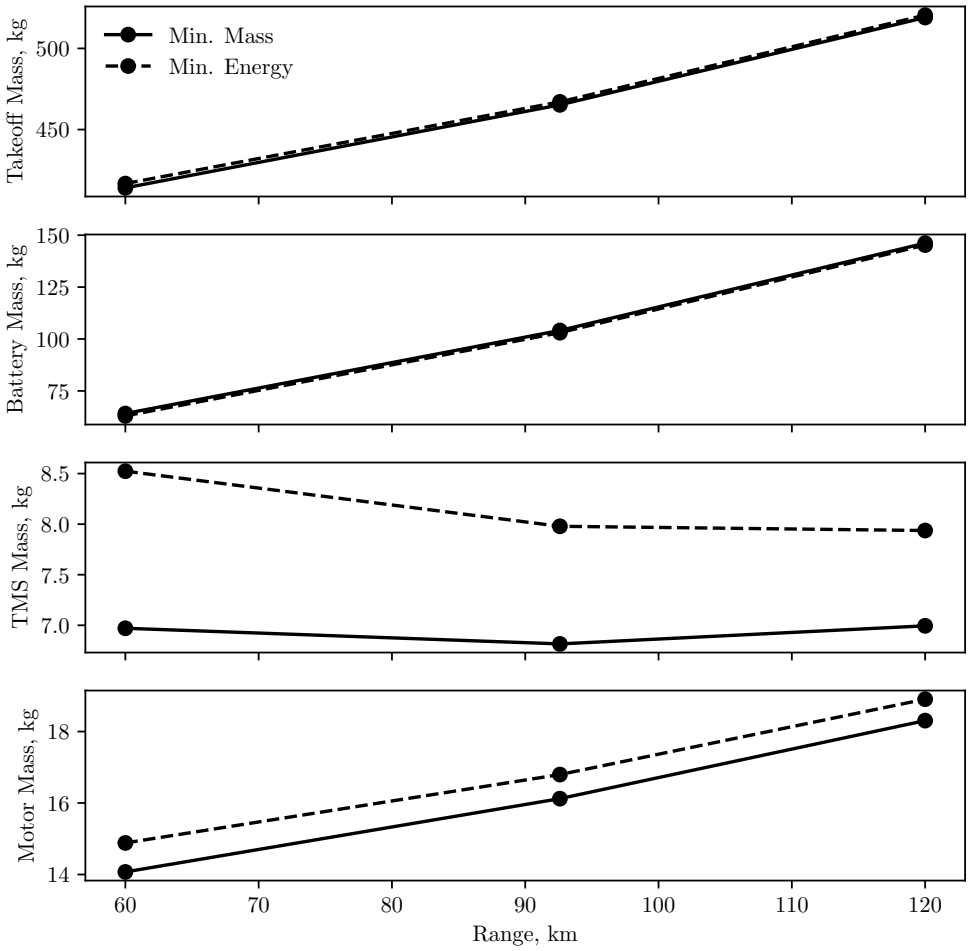

Figure 10: Aircraft Mass Characteristics at Different Mission Ranges.

in the designs between these two objectives. Most notably, the minimum energy vehicles optimize to a slightly heavier takeoff mass design despite having a slightly lower battery mass as less energy needs to be stored. For the minimum energy objective, the optimizer found that slightly larger, more powerful motors as well as a larger TMS were beneficial compared to the minimum mass cases. Essentially, the optimizer traded increased motor and TMS mass for reduced TMS power and mission time to reduce the overall energy consumption.

The results provided in Table 2 and Fig. 10 provide an overview of how the different objective functions and range requirements change the physical vehicle design. Within the design environment created for this research however, the mission trajectory and operating behavior of the various systems are also determined as part of the optimization problem. The resulting mission trajectory and operating characteristics for notable subsystems are shown in Fig. 11 providing further insights into the optimal design of these UAM concepts.

The second plot of Fig. 11 shows the motor power (average of front and rear motors) profile throughout the flight. In this plot, it is clear that the minimum energy objective function cases have more powerful motors compared to the minimum mass cases at the same range. While these more powerful motors are needed to lift the slightly heavier vehicle in the minimum energy cases, the extra power is applied over a shorter period of time to fly faster leading to an significant decrease in flight time for the same range.

With this power profile throughout the flight, the optimal trajectories flown by each of the vehicles considered in this study are shown in the top plot. For each of the cases, the aircraft initially climbs to a minimum cruise altitude which was assumed to be 1700 m. After reaching this cruise altitude, each of the trajectories follow this lower bound for a while as the optimizer determined it was ineffective to spend additional energy to reach a higher altitude. However, part way through the flight, each of the vehicles starts to climb to a higher altitude before descending and landing. While this trajectory may not seem logical or desirable for a real flight, it was consistently determined by the optimizer to be the best combination of trajectory and vehicle design for the quadrotor concept due to the thermal constraints on the battery.

As shown in the third plot of Fig. 11, in each study the battery was assumed to start at the ambient hot day temperature of 35 °C. For approximately the first half of each of trajectories, the aircraft climbed at maximum power then pitched over and maintained a minimum cruise altitude (1700 m). During this time, the high power draw causes the battery temperature to slowly heat up despite the cooling provided by the TMS. While the aircraft would prefer to stay at this low cruise altitude, the continual increase in battery temperature would require a larger TMS to stay under the temperature limit. Rather than increase the TMS size (and weight), the preferred solution with the selected objective functions is to instead have the vehicle climb to a higher altitude starting about halfway through the flight. This climb is achieved by maintaining the maximum power and decreasing the aircraft pitch such that more thrust is going in the vertical direction. By increasing altitude, two things are achieved. First, the TMS gains a slight performance benefit from colder ambient air passing through the heat exchanger. Second, and probably more importantly, this trajectory allows the aircraft to hit the maximum temperature and highest altitude around the same time. Once this limit is reached, the rotor thrust and battery power draw can be reduced for descent and as a means to lower the heat generated in the battery. This control approach provides a way to alter the operation of the vehicle without having to increase the size of the TMS to handle the heat loads generated by the electrical power system especially during descent. The impact of this thermal constraint is further demonstrated in the studies in the next section.

B. Maximum Battery Temperature Design Study

To further study the thermal constraints on the quadrotor vehicle, a set of optimization studies were conducted which varied the allowable battery temperature. In addition to the baseline 50 °C constraint used in the previous section, limits of 40 °C and 60 °C were considered with optimizations completed using both minimum energy and minimum mass objective functions. (Note that all cases in this section were run with the nominal 92.6km mission.) The results from these studies are summarized in Table 3 with mass trends shown in Fig. 12.

Overall, the six designs evaluated with different thermal constraints produced fairly similar aircraft designs with the takeoff mass of the vehicles being within approximately 10 kg of each other (<2.5% difference). As anticipated, the takeoff mass trend decreases with higher allowable battery temperatures as a result of smaller TMS being required to dissipate the heat generated. Along with this trend in reduced TMS mass, the battery mass and motor mass also decrease slightly with the increased allowable battery temperatures as a result of a lighter vehicle and lower power requirements. Finally, Fig. 12 shows similar results when comparing the minimum energy and minimum mass objective functions. The minimum energy cases tend

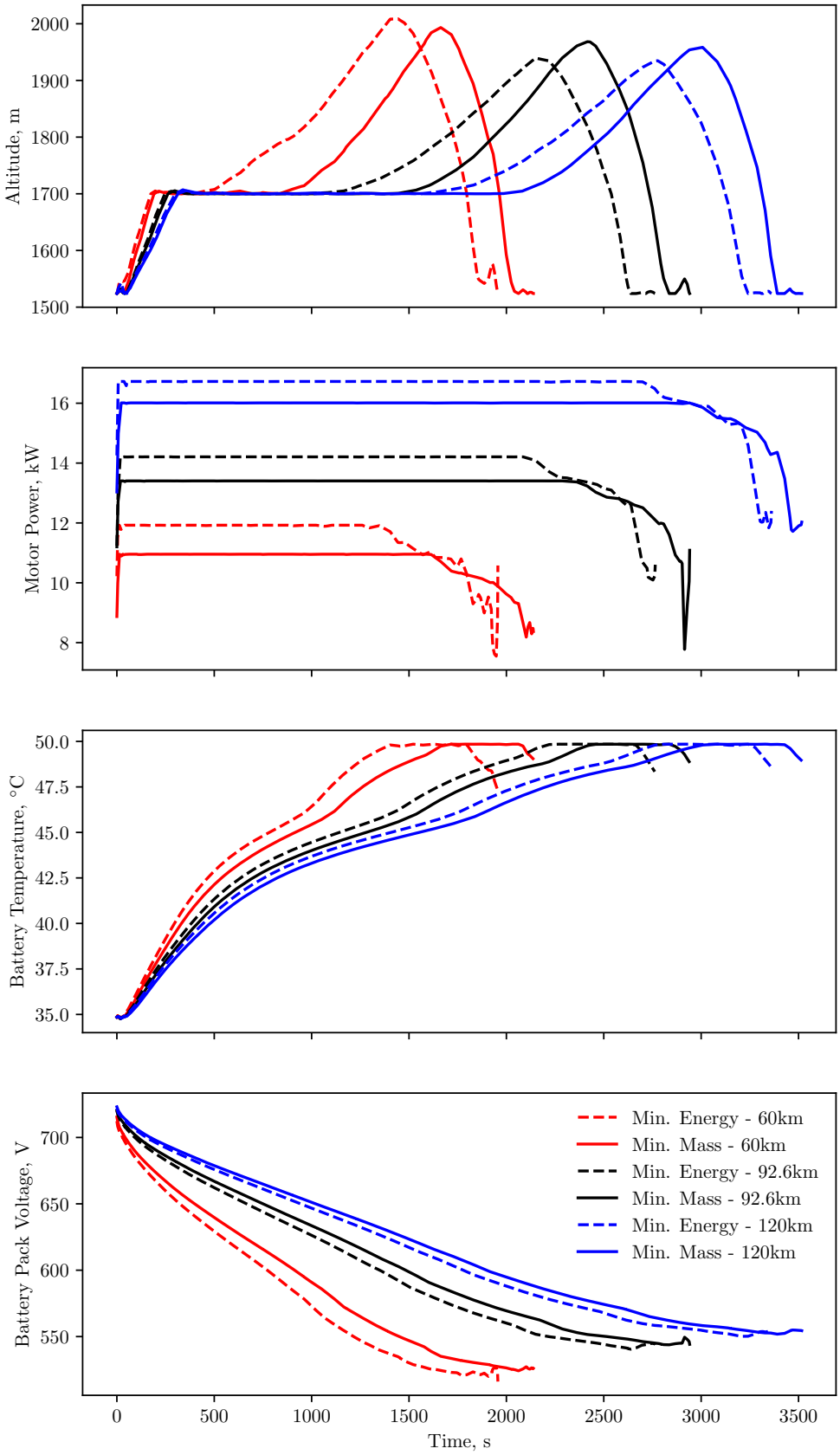

Figure 11: Aircraft Performance Characteristics at Different Mission Ranges.

Table 3: Vehicle Design Characteristics at Different Max Allowable Battery Temperatures.

System	Parameter	Min. Energy 40C	Min. Mass 40C	Min. Energy 50C	Min. Mass 50C	Min. Energy 60C	Min. Mass 60C
Vehicle	Range, km	92.6	92.6	92.6	92.6	92.6	92.6
	Takeoff Mass, kg	473.20	471.05	467.07	465.23	464.09	462.52
Battery	Max Temp, °C	39.85	39.85	49.85	49.85	59.85	59.85
	Total Energy, kWh	52.78	53.43	51.56	52.09	51.08	51.61
	Max Cell Discharge, A	4.24	4.01	4.21	3.95	4.18	3.92
	Energy Density, Wh/kg	400	400	400	400	400	400
	Mass, kg	105.48	106.78	103.04	104.10	102.07	103.14
TMS	Max Power, kW	0.86	1.11	0.57	0.76	0.45	0.63
	HX Width, m	0.353	0.246	0.233	0.167	0.185	0.143
	HX Height (Coolant), m	0.027	0.025	0.027	0.026	0.025	0.023
	HX Height (Air), m	0.500	0.500	0.500	0.500	0.500	0.500
	Mass, kg	10.20	8.41	7.98	6.82	6.70	5.76
Motors	Shaft Power, kW	14.63	13.89	14.21	13.40	14.01	13.21
	Mass, kg	4.29	4.13	4.20	4.03	4.16	3.99
Rotors	Diameter, m	3.66	3.66	3.66	3.66	3.66	3.66

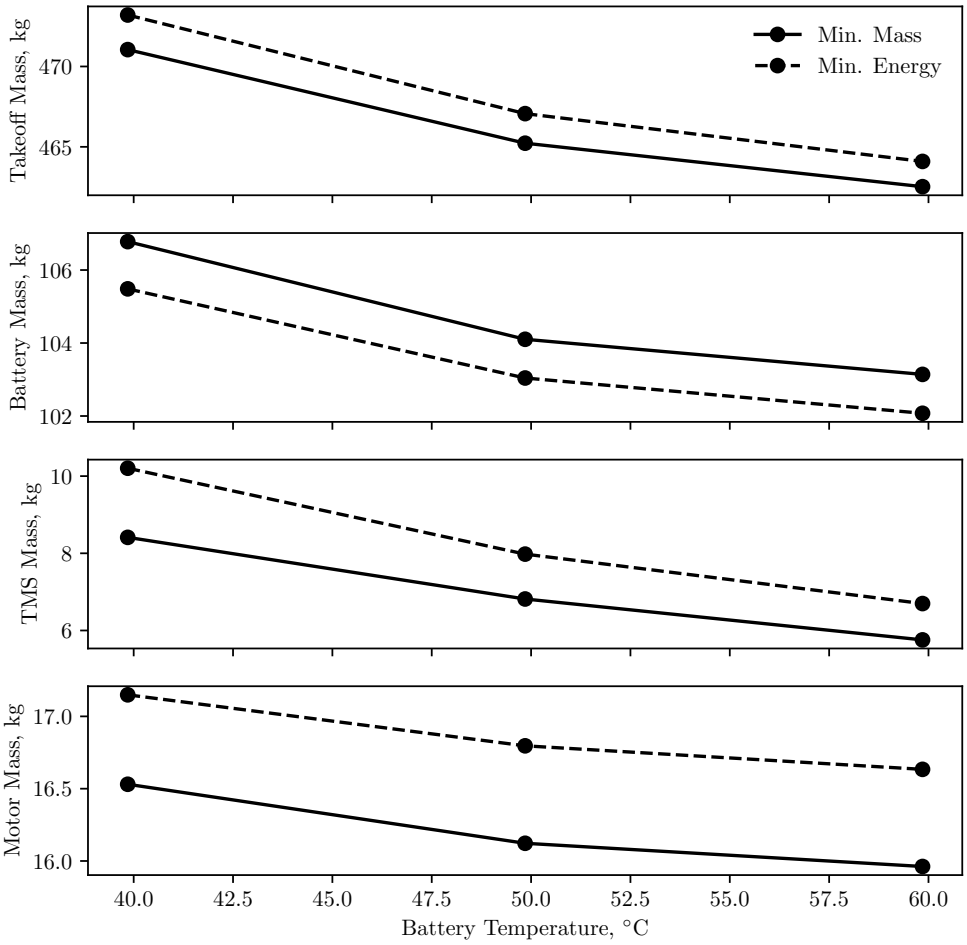

Figure 12: Aircraft Mass Characteristics at Different Max Allowable Battery Temperatures.

towards heavier takeoff mass vehicles by a few kilograms with larger motors and TMS, but have reduce battery mass.

While changing the battery temperature constraints had a minimal impact on the overall mass of the vehicle, these changes did have a more pronounced impact on the optimal operation of these designs as shown in Fig. 13. In the third plot from the top, the impact of the different constraints can clearly be observed in the time history of the battery temperature. For the 40 °C limited case, the battery quickly approaches the constraint and spends a significant portion of the flight in a steady-state temperature. Meanwhile, cases with higher temperature limits spend less time operating at this constraint.

In addition to the changes in the temperature time history, the different battery temperature constraints significantly impacted the optimal trajectory flown by each design as shown in the top plot of Fig. 13. Similar to the results shown in the mission range study, the trajectories in the present studies depict a climb to higher altitudes partway through the flight. These climbs again allow for cooler air to pass through the heat exchanger and for lower power draws during descent when the battery temperature is limiting. For the 40 °C constrained case, the lower temperature constraint results in the aircraft starting to climb earlier in the mission and reaching a high altitude. This allows for a longer descent at reduced power when the temperature is a limiting factor. In comparison, for the 60 °C case, the aircraft can stay at the minimum cruise altitude for almost the entire flight with only a small increase in altitude required at the very end to best fulfill the design objective while satisfying the battery temperature constraints.

IV. Conclusion

The concept of UAM provides an opportunity to augment current urban transportation systems, allowing passengers to avoid street traffic by taking advantage of the airspace over a city. This emerging market has garnered significant commercial interest, with various entities proposing a wide range of vehicle designs to fill anticipated mission requirements. Given the shorter flights expected in this market as well as the need for lower environmental impact, many of these vehicle concepts are exploring the use of unconventional aircraft configurations which utilize new technologies such as electric propulsion systems. While these new technologies and configurations are promising, they also present additional challenges in the design process as traditional design tools are often incapable of modeling some subsystems and do not capture important interactions between them.

This paper presented the continued development of a multidisciplinary design optimization environment for developing UAM concept vehicles, specifically those with all-electric propulsion systems. These systems present challenges particularly in regard to the electric propulsion system design and the need for a thermal management system to make sure the electric components stay at appropriate temperatures. The developed multidisciplinary design optimization capability, presented in Section II, includes models for most of the major subsystems required for these vehicles including the rotor, electric motors, cable, batteries, thermal management system, and flight dynamics. These disciplinary analyses are tightly couple together to ensure an optimal, yet valid, design is developed during the design process. In addition, the implemented design methodology allows for both the vehicle and its flight path to be designed simultaneously, thereby allowing the optimizer to find the best solution with a wide range of design variables to satisfy the desired requirements and constraints.

Using the developed multidisciplinary environment, a number of demonstration design studies were completed using an all-electric quadrotor concept. In these design studies, design characteristics such as the mission range, allowable battery temperature, battery energy density and rotor diameter were varied, with each case going through the optimization process. Furthermore, two different objective functions were considered to explore differences resulting from minimizing energy usage compared to minimizing vehicle mass. The results from these demonstration studies revealed several interesting conclusions.

First, the design optimization reduced the size of TMS to reduce weight and energy usage. To meet thermal constraints on battery temperature, the optimal solution prefers to alter the flight path to satisfy constraints by gaining altitude such that the aircraft reaches peak altitude at the battery maximum temperature just before starting descent at the end of the flight. This trajectory may not ultimately be realistic for actual flights, but this result demonstrates the interactions which are captured by this tightly coupled multidisciplinary modeling approach which should be considered early in the design process. Failure to consider these interactions to lead to under or over designed components which can later impact the allowable mission performance envelope.

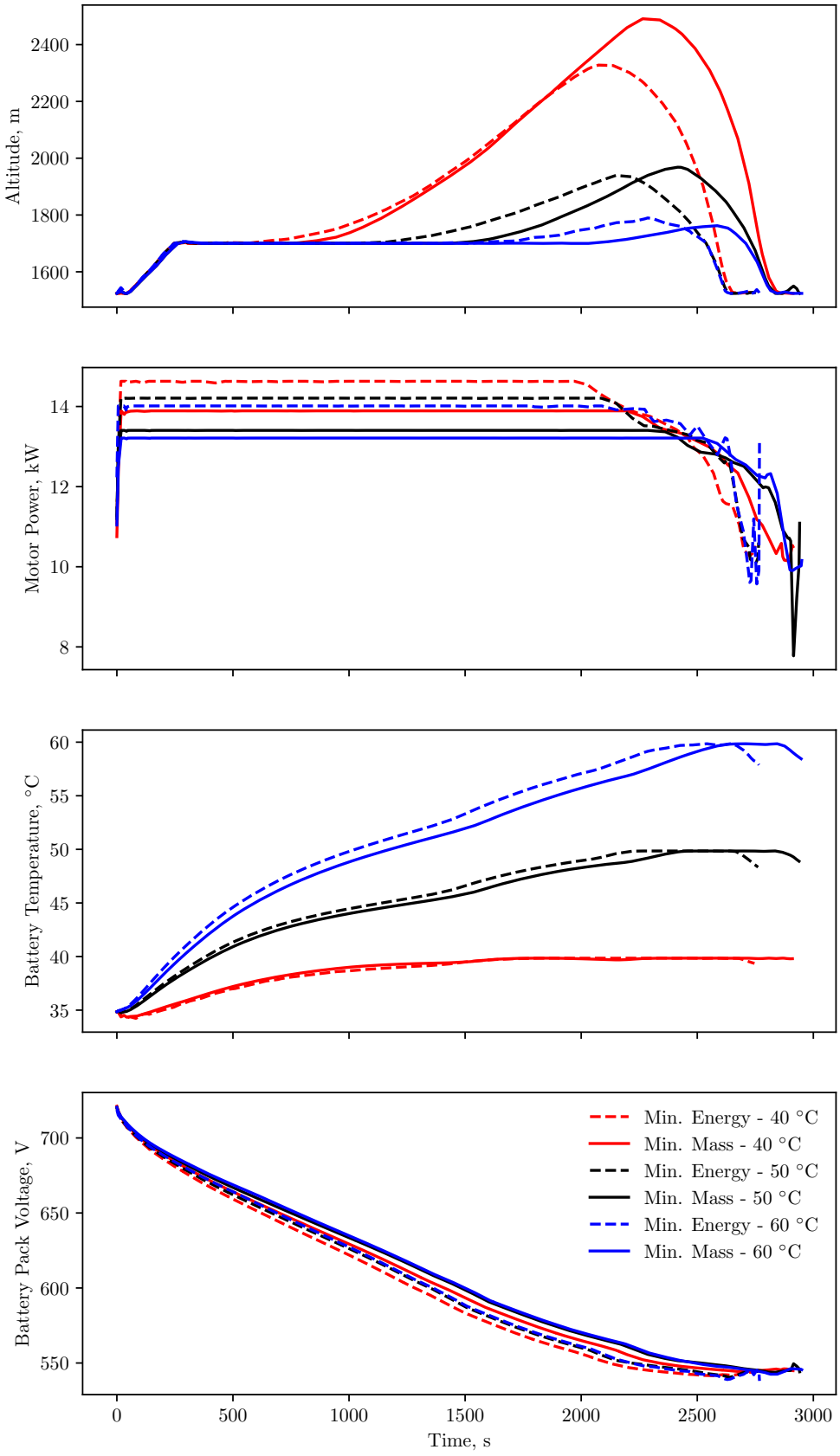

Figure 13: Aircraft Performance Characteristics at Different Max Allowable Battery Temperatures.

Second, to further explore the impact of the thermal constraints on the vehicle design and operation, a battery temperature design study was completed. This studies showed that increasing cooling of the battery (by enforcing lower temperature limits) resulted in only a minor increase in the TMS and total aircraft mass. However, the decrease in allowable battery temperature also impacted the flight path with the aircraft needing to climb to higher altitudes. In comparison, lowering the cooling requirements by allowing the battery to reach higher temperatures significantly reduced the need to climb in flight. These trades show the importance the battery temperature limits and TMS sizing will play in the eventual design of electric UAM vehicles as well as the need to properly constrain the allowable flight path.

Finally, across all the studies presented in this paper both minimum energy and minimum mass objective functions were considered. In general, these two objectives produced similar results with only slight differences in the vehicle design. The minimum energy cases always optimized to a slightly heavier aircraft with more powerful motors and TMS, but with lighter batteries. This trade allowed the vehicle to fly faster to the destination while climbing to a slightly lower peak altitude before descending thereby slightly reducing the total energy used. In every case, the vehicle optimized to the minimum possible battery size, with the aircraft ending each flight with a 20% battery state of charge.

In total, the results presented in this this paper demonstrate the current potential of multidisciplinary analysis environment for analyzing UAM concepts. These results show the vehicle can trade some increase in vehicle mass to reduce overall mission energy. This trade is important as vehicle mass often is related to development/manufacturing costs, while energy use is related to operating costs. This additional optimization capability looking at both the physical vehicle design and operation further helps make informed decisions.

While the completed studies show important design tradeoffs which must be considered, there is additional work needed to enhanced this capability for future studies. Primarily, the future work needs to explore the integration of higher fidelity models for many of the subsystems, specifically the rotor and motor. In the present work, the rotors were modeled as individual, isolated systems to compute the thrust and power. However, there will be interactions between the wakes of the rotors in this quadrotor configuration which can effect performance that will need to be captured. Beyond the performance impacts, the interactions between the rotors will also impact the noise produced by the aircraft. Given the operation of these vehicles in densely populated urban environments, the acoustics of the aircraft need to be analyzed as part of the multidisciplinary process and will likely impact the trajectory selected. Adding additional fidelity to these models and incorporating the acoustic analysis will provide a better design capability and provide further insights into the coupling between disciplines which must be considered for unconventional UAM systems.

Appendix

A. Battery Energy Density and Rotor Diameter Design Studies

Two additional design optimization studies were conducted to explore other aspects of the quadrotor design space. The first of these studies considered the impact of battery technology in the form of the available energy density of the battery cells and pack. The studies shown throughout the rest of the paper assumed an energy density of 400 Wh/kg. However, this energy density is not available with current battery technology levels so two lower energy density assumptions were evaluated: 300 Wh/kg and 350 Wh/kg.

The results from these battery energy density studies for both objective functions are provided in Table 4 as well as Figures 14 and 15. For the electric quadrotor concepts studied here, the battery mass is a significant portion of the overall vehicle mass comprising upwards of 20% of the takeoff mass. As a result, any change in the energy density significantly impacts the overall weight of the battery and has a further effect on the weight of other vehicle subsystems. As shown in Fig. 14, the overall aircraft mass increases substantially for the lower battery energy densities with most of the increase coming from the battery mass. The impact on the motor mass and TMS mass are smaller with increases of only a few kilograms at lower energy densities.

Despite the significant changes in the mass of the generated designs as a function of battery energy density, Fig. 15 shows only minor variations in the optimal trajectory for the designs. Each of the vehicles start the climb to avoid the temperature constraint around the same point in the flight and reach about the same altitude. The biggest difference between the different designs in this study is the motor power profiles as the lower energy density cases require higher power levels throughout the flight which is expected given the heavier vehicle.

The last study completed in this research effort was to explore different rotor diameters for the vehicle.

Table 4: Vehicle Design Characteristics at Different Battery Energy Densities.

System	Parameter	Min. Energy 300kWh/kg	Min. Mass 300kWh/kg	Min. Energy 350kWh/kg	Min. Mass 350kWh/kg	Min. Energy 400kWh/kg	Min. Mass 400kWh/kg
Vehicle	Range, km	92.6	92.6	92.6	92.6	92.6	92.6
	Takeoff Mass, kg	539.28	537.81	495.49	493.89	467.07	465.23
Battery	Max Temp, °C	49.85	49.85	49.85	49.85	49.85	49.85
	Total Energy, kWh	59.75	60.05	54.74	55.28	51.56	52.09
	Max Cell Discharge, A	4.43	4.26	4.31	4.08	4.21	3.95
	Energy Density, Wh/kg	300	300	350	350	400	400
	Mass, kg	159.32	160.13	125.08	126.32	103.04	104.10
TMS	Max Power, kW	0.75	0.92	0.64	0.90	0.57	0.76
	HX Width, m	0.286	0.229	0.256	0.218	0.233	0.167
	HX Height (Coolant), m	0.027	0.026	0.027	0.023	0.027	0.026
	HX Height (Air), m	0.500	0.500	0.500	0.500	0.500	0.500
	Mass, kg	9.02	8.05	8.42	7.16	7.98	6.82
Motors	Shaft Power, kW	17.44	16.80	15.49	14.73	14.21	13.40
	Mass, kg	4.87	4.74	4.47	4.31	4.20	4.03
Rotors	Diameter, m	3.66	3.66	3.66	3.66	3.66	3.66

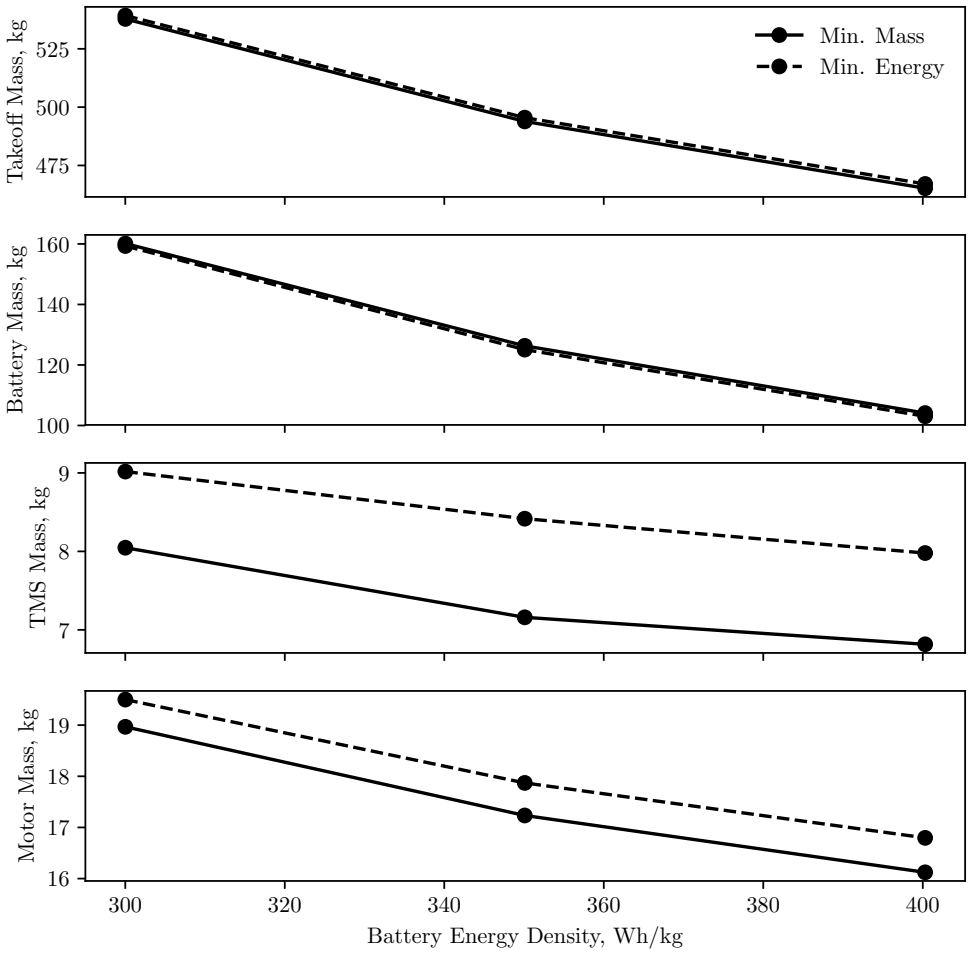

Figure 14: Aircraft Mass Characteristics at Different Battery Energy Densities.

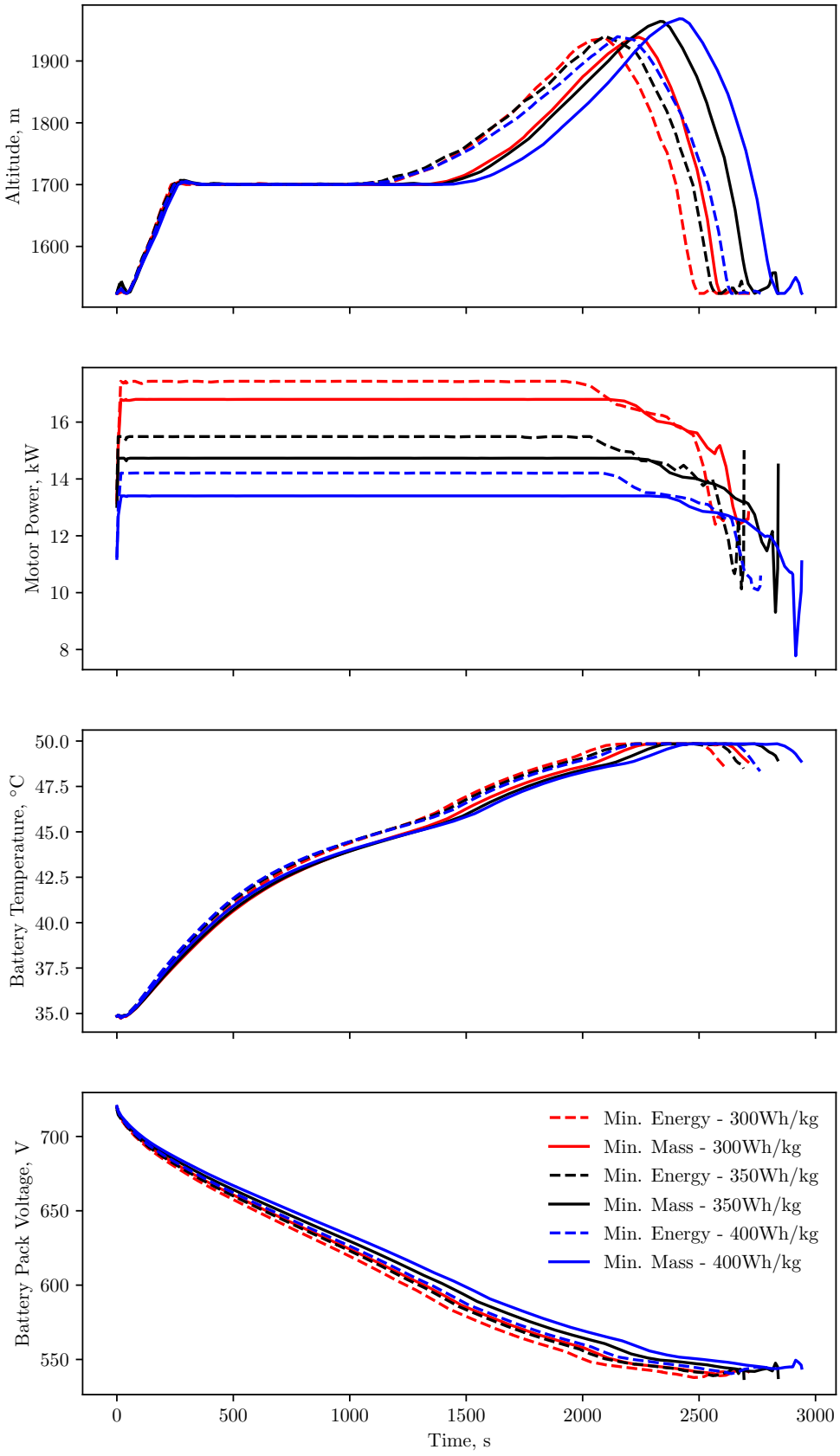

Figure 15: Aircraft Performance Characteristics at Different Battery Energy Densities.

This value was held constant throughout the previous studies at 3.66 m, which is similar to the values determined in the initial conceptual design.[3] This study explored the impact of a smaller (3.3 m) and larger (4.0 m) rotor diameter on the overall vehicle design.

The vehicle design characteristics and mass trends are shown in Table 5 and Fig. 16, respectively. From these results, it can be seen that the smaller rotors, while weighing less themselves, result in a slightly heavier aircraft overall (less than a 10 kg difference within the diameters selected). In addition to changes to diameter, the airfoil twist distribution along the blades is being redesigned in each of these optimizations resulting in different rotor efficiencies. These rotor efficiency changes in both hover and cruise also contribute to the need for more powerful motors, larger batteries, and a larger TMS on the aircraft. The increased motor power with rotor diameter can be observed in Fig. 17. While the rotor diameter has only a minor impact on aircraft weight, Fig. 17 also reveals that the rotor diameter does impact the optimal trajectory as the lower rotor diameter cases have shorter flight times to complete the same mission. Although these flights are shorter, the decrease in rotor efficiency and increased power for the smaller rotor cases results in higher total energy requirements.

Table 5: Vehicle Design Characteristics at Different Rotor Diameters.

System	**Parameter**	**Min. Energy 3.3m**	**Min. Mass 3.3m**	**Min. Energy 3.7m**	**Min. Mass 3.7m**	**Min. Energy 4.0m**	**Min. Mass 4.0m**
Vehicle	Range, km	92.6	92.6	92.6	92.6	92.6	92.6
	Takeoff Mass, kg	474.00	471.38	467.07	465.23	464.30	462.52
Battery	Max Temp, °C	49.85	49.85	49.85	49.85	49.85	49.85
	Total Energy, kWh	55.87	56.00	51.56	52.09	48.49	49.13
	Max Cell Discharge, A	4.35	4.08	4.21	3.95	4.09	3.82
	Energy Density, Wh/kg	400	400	400	400	400	400
	Mass, kg	111.65	111.91	103.04	104.10	96.91	98.18
TMS	Max Power, kW	0.68	0.87	0.57	0.76	0.51	0.74
	HX Width, m	0.260	0.189	0.233	0.167	0.213	0.172
	HX Height (Coolant), m	0.027	0.026	0.027	0.026	0.027	0.023
	HX Height (Air), m	0.500	0.500	0.500	0.500	0.500	0.500
	Mass, kg	8.51	7.28	7.98	6.82	7.57	6.30
Motors	Shaft Power, kW	15.97	14.93	14.21	13.40	12.97	12.19
	Mass, kg	4.57	4.35	4.20	4.03	3.94	3.78
Rotors	Diameter, m	3.30	3.33	3.66	3.66	4.00	4.00

Overall, the two additional studies described in this section show the design trends for just a few of the assumptions made regarding the quadrotor configuration using the developed modeling environment. These studies capture important sensitivities of the vehicle mass to these inputs, but also revealed that those design changes had a limited impact on the optimal trajectory to be flown by the vehicle.

Acknowledgements

The work presented in this paper was supported by NASA's Transformational Tools and Technologies (TTT) Project with information about the conceptual quadrotor UAM design provided by NASA's Revolutionary Vertical Lift Technology (RVLT) Project.

References

[1]Hasan, S., "Urban Air Mobility (UAM) Market Study," Tech. rep., NASA, March 2019, HQ-E-DAA-TN63497.

[2]Goyal, R., "Urban Air Mobility (UAM) Market Study," Tech. rep., NASA, March 2019, HQ-E-DAA-TN65181.

[3]Johnson, W., Silva, C., and Solis, E., "Concept Vehicles for VTOL Air Taxi Operations," *AHS Technical Conference on Aeromechanics Design for Transformative Vertical Flight*, AHS, San Francisco, January 2018.

[4]Silva, C., Johnson, W., Solis, E., Patterson, M., and Antcliff, K., "VTOL Urban Air Mobility Concept Vehicles for Technology Development," *AIAA Aviation 2018 Forum*, AIAA, June 2018, AIAA paper 2018-3847.

[5]Hendricks, E., Falk, R., Gray, J., Aretskin-Hariton, E., Ingraham, D., Chapman, J., Schnulo, S., Chin, J., Jasa, J., and Bergeson, J., "Multidisciplinary Optimization of a Turboelectric Tiltwing Urban Air Mobility Aircraft," *AIAA Aviation 2019 Forum*, AIAA, June 2019, AIAA paper 2019-3551.

[6]Hendricks, E. S., Aretskin-Hariton, E., Chapman, J. W., Gray, J. S., and Falck, R. D., "Propulsion System Optimization for a Turboelectric Tiltwing Urban Air Mobility Aircraft," *ISABE 2019*, ISABE, Canberra, Australia, 2019.

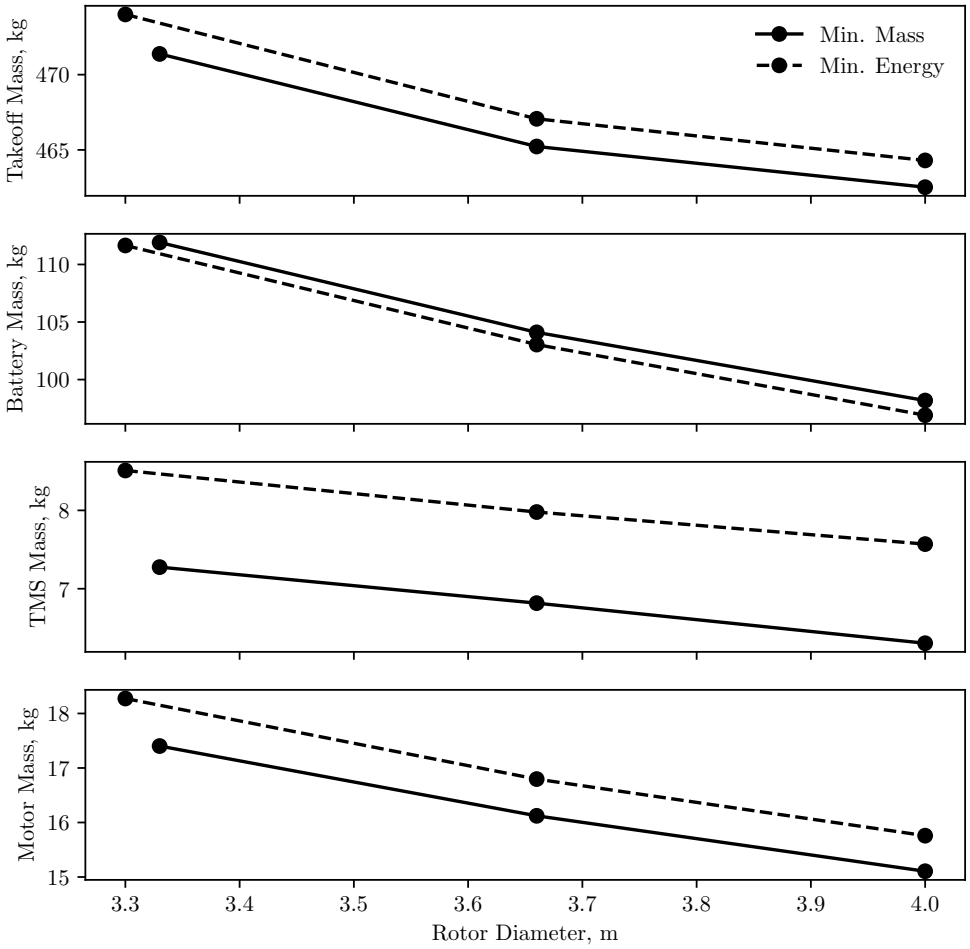

Figure 16: Aircraft Mass Characteristics at Different Rotor Diameters.

[7]Lambe, A. B. and Martins, J. R. R. A., "Extensions to the Design Structure Matrix for the Description of Multidisciplinary Design, Analysis, and Optimization Processes," *Structural and Multidisciplinary Optimization*, Vol. 46, 2012, pp. 273–284.

[8]Gray, J. S., Hwang, J. T., Martins, J. R. R. A., Moore, K. T., and Naylor, B. A., "OpenMDAO: An Open-Source Framework for Multidisciplinary Design, Analysis, and Optimization," *Structural and Multidisciplinary Optimization*, Vol. 59, 2019, pp. 1075–1104.

[9]Falck, R. D. and Gray, J. S., "Optimal Control within the Context of Multidisciplinary Design, Analysis, and Optimization," *AIAA Scitech 2019 Forum*, AIAA, 2019, AIAA paper 2019-0976.

[10]Leishman, J. G., *Principles of Helicopter Aerodynamics*, No. 18 in Cambridge Aerospace Series, Cambridge University Press, Cambridge ; New York, 2nd ed., 2006, OCLC: ocm61463625.

[11]Manwell, J. F., McGowan, J. G., and Rogers, A. L., *Wind Energy Explained: Theory, Design and Application*, Wiley, Chichester, U.K, 2nd ed., 2009, OCLC: ocn431936159.

[12]Hansen, M. O. L., *Aerodynamics of Wind Turbines*, Earthscan Publications Ltd., jan 2008.

[13]Burton, T., editor, *Wind Energy Handbook*, J. Wiley, Chichester ; New York, 2001.

[14]Andrew Ning, S., "A Simple Solution Method for the Blade Element Momentum Equations with Guaranteed Convergence," *Wind Energy*, Vol. 17, No. 9, Sept. 2014, pp. 1327–1345.

[15]Ning, S. A., "CCBlade.jl," May 2020, `https://github.com/byuflowlab/ccblade.jl`.

[16]Ning, S. A., "CCBlade," May 2013, `https://www.osti.gov//servlets/purl/1262682`.

[17]"The Julia Language," `https://julialang.org/`.

[18]Ning, S. A. and McDonnell, T., "FLOWMath.jl," 5 2020, `https://github.com/byuflowlab/FLOWMath.jl`.

[19]Revels, J., Lubin, M., and Papamarkou, T., "Forward-Mode Automatic Differentiation in Julia," *CoRR*, Vol. abs/1607.07892, April 2016, `https://arxiv.org/abs/1607.07892`.

[20]Johnson, W., "NASA Design and Analysis of Rotorcraft Theory Manual," 2012, `https://rotorcraft.arc.nasa.gov/Publications/files/NDARCTheory_v1_6_938.pdf`.

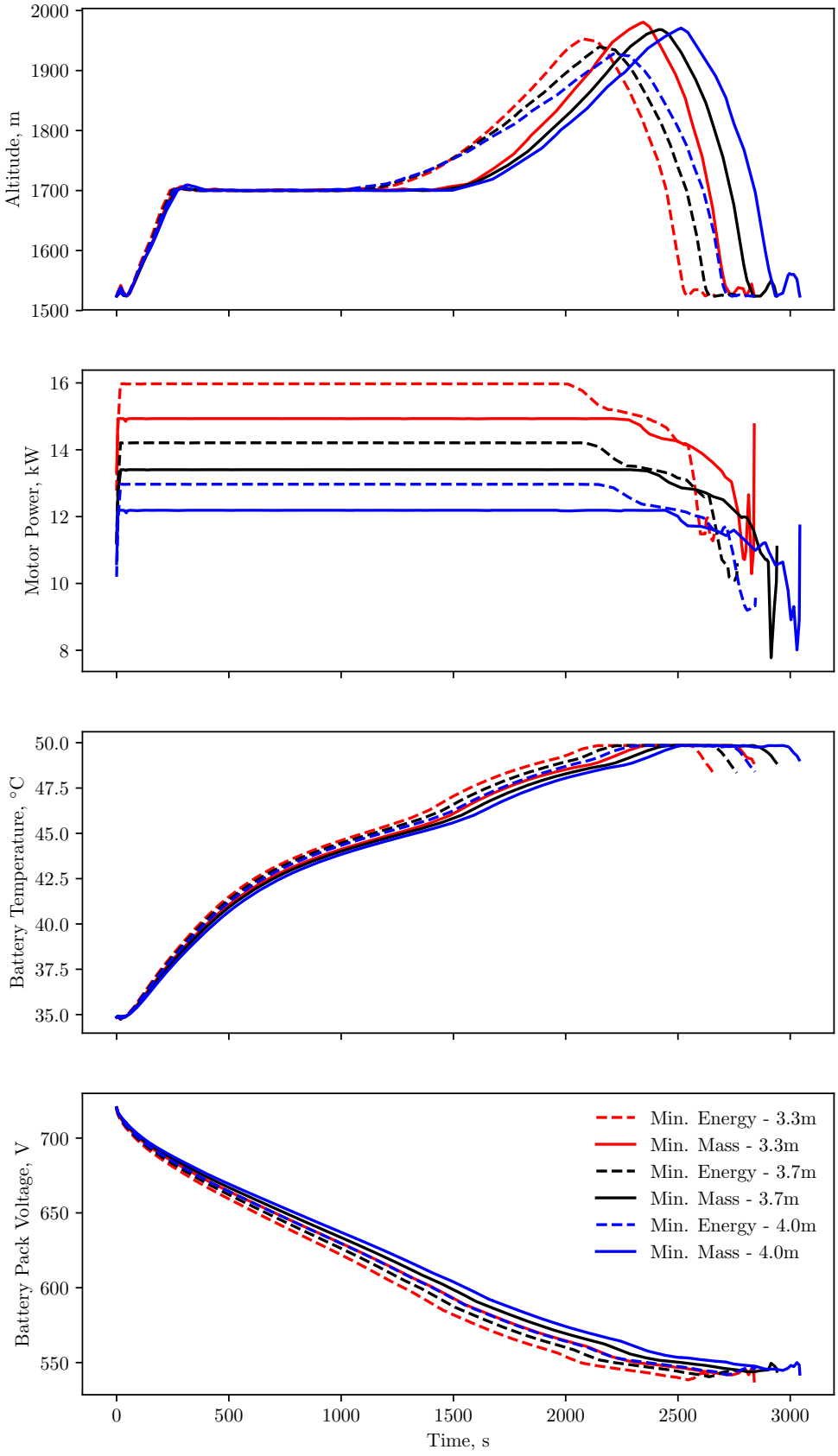

Figure 17: Aircraft Performance Characteristics at Different Rotor Diameters.

[21]Brown, G., Kascak, A., Ebihara, B., Johnson, D., Choi, B., Siebert, M., and Buccieri, C., "NASA Glenn Research Center Program in High Power Density Motors for Aeropropulsion," Tech. rep., NASA, December 2005, NASA TM-2005-213800.

[22]Hendricks, E., Chapman, J., and Aretskin-Hariton, E., "Load Flow Analysis with Analytic Derivatives for Electric Aircraft Design Optimization," *AIAA Scitech 2019 Forum*, January 2019, AIAA paper 2019-1220.

[23]Aretskin-Hariton, E., Schnulo, S., Hendricks, E., and Chapman, J., "Electrical Cable Design for Urban Air Mobility," *AIAA SciTech 2020 Forum*, AIAA, January 2020, AIAA paper 2020-0014.

[24]Chin, J., Schnulo, S., Miller, T., Prokopius, K., and Gray, J., "Battery Performance Modeling on SCEPTOR X-57 Subject to Thermal and Transient Considerations," *AIAA SciTech 2019 Forum*, AIAA, January 2019, AIAA paper 2019-0784.

[25]Chapman, J., Schnulo, S., and Nitsche, M., "Development of a Thermal Management System for Electrified Aircraft," *AIAA Scitech 2020 Forum*, AIAA, January 2020, AIAA paper 2020-0545.

[26]Beard, R., "Quadrotor Dynamics and Control Rev 0.1," 2008.